Essential functions of Sds22p in chromosome stability and nuclear localization of PP1

Mark W. Peggie[1], Sarah H. MacKelvie[1,*], Andrew Bloecher[2,‡], Elena V. Knatko[1], Kelly Tatchell[2] and Michael J. R. Stark[1,§]

[1]Division of Gene Regulation and Expression, School of Life Sciences, MSI/WTB Complex, University of Dundee, Dundee, DD1 5EH, UK
[2]Department of Biochemistry and Molecular Biology, Louisiana State University Health Sciences Center, Shreveport, LA 71130, USA
*Present address: Scottish Enterprise Tayside, 45 North Lindsay Street, Dundee, DD1 1HT, UK
‡Present address: Fred Hutchinson Cancer Research Center, Division of Basic Research, 1100 Fairview Avenue North, Seattle, WA 98109, USA
§Author for correspondence (e-mail: m.j.r.stark@dundee.ac.uk)

Accepted 19 September 2001
Journal of Cell Science 115, 195-206 (2002) © The Company of Biologists Ltd

Summary

Sds22p is a conserved, leucine-rich repeat protein that interacts with the catalytic subunit of protein phosphatase 1 ($PP1_C$) and which has been proposed to regulate one or more functions of $PP1_C$ during mitosis. Here we show that *Saccharomyces cerevisiae* Sds22p is a largely nuclear protein, most of which is present as a stable 1:1 complex with yeast $PP1_C$ (Glc7p). Temperature-sensitive (Ts^-) *S. cerevisiae sds22* mutants show profound chromosome instability at elevated growth temperatures but do not confer a cell cycle stage-specific arrest. In the *sds22-6* Ts^- mutant, nuclear Glc7p is both reduced in level and aberrantly localized at 37°C and the interaction between Glc7p and Sds22p in vitro is reduced at higher temperatures, consistent with the in vivo Ts^- growth defect. Like some *glc7* mutations, *sds22-6* can suppress the Ts^- growth defect associated with *ipl1-2*, a loss of function mutation in a protein kinase that is known to work in opposition to PP1 on at least two nuclear substrates. This, together with reciprocal genetic interactions between *GLC7* and *SDS22*, suggests that Sds22p functions positively with Glc7p to promote dephosphorylation of nuclear substrates required for faithful transmission of chromosomes during mitosis, and this role is at least partly mediated by effects of Sds22p on the nuclear distribution of Glc7p

Key words: Protein phosphatase 1, *SDS22*, *GLC7*

Introduction

Type 1 protein phosphatase (PP1) is a highly conserved member of the PPP family of protein serine-threonine phosphatases that plays important roles in a wide range of cellular functions. In the budding yeast *Saccharomyces cerevisiae* the essential gene *GLC7* encodes the catalytic subunit of PP1. A variety of studies using *glc7* mutants have revealed that yeast PP1 is required for many key cellular functions including glucose repression (Tu and Carlson, 1994; Tu and Carlson, 1995), kinetochore function (Bloecher and Tatchell, 1999; Sassoon et al., 1999), vesicle fusion during protein secretion (Peters et al., 1999), glycogen synthesis (Feng et al., 1991), meiosis (Bailis and Roeder, 2000; Tu et al., 1996) and cell wall integrity (Andrews and Stark, 2000). Rather than acting on its own, the catalytic subunit of PP1 ($PP1_C$) has been found to interact with proteins that regulate specific PP1 dephosphorylation events (Hubbard and Cohen, 1993; Bollen, 2001). For example, mammalian PP1 has been shown to bind tissue-specific glycogen-binding subunits such as G_L, and G_M, which target the enzyme to glycogen particles where it can dephosphorylate key enzymes of glycogen metabolism such as glycogen synthase (Doherty et al., 1995; Hubbard and Cohen, 1989). In *S. cerevisiae*, a related protein (Gac1p) performs a similar function and is required for PP1 to activate glycogen synthase by dephosphorylation (François et al., 1992; Stuart et al., 1994), while Reg1p is involved in the roles of PP1 in glucose repression and glucose signalling (Frederick and Tatchell, 1996; Jiang et al., 2000; Tu and Carlson, 1995). In budding yeast, over a dozen proteins have been demonstrated or proposed to interact with $PP1_C$ (Stark, 1996; Uetz et al., 2000), while other $PP1_C$-interacting proteins known in higher eukaryotes include regulatory subunits that target PP1 to myosin (Alessi et al., 1992) or that form complexes with $PP1_C$ in the nucleus (Ajuh et al., 2000; Allen et al., 1998; Kreivi et al., 1997; Van Eynde et al., 1995). A conserved motif of the form -V/IXF- has been identified that mediates the interaction between $PP1_C$ and many of its regulatory subunits (Egloff et al., 1997; Zhao and Lee, 1997).

SDS22 is the budding yeast homologue of *Schizosaccharomyces pombe sds22*$^+$ (Hisamoto et al., 1995; MacKelvie et al., 1995). *S. pombe* Sds22 is a nuclear protein that binds directly to the catalytic subunit of PP1 and which largely consists of 11 tandem leucine-rich repeats (Stone et al., 1993), although it lacks the -V/IXF- motif found in many $PP1_C$-interacting proteins. The corresponding gene (*sds22*$^+$) was isolated as a high-copy suppressor of a conditional mutation (*dis2-11*) affecting the major fission yeast PP1 catalytic subunit Dis2 (Ohkura and Yanagida, 1991). A temperature-sensitive *sds22* allele led to a metaphase-like arrest of fission yeast cells at the restrictive temperature, with high histone H1 kinase activity, a short spindle and condensed chromosomes (Stone et al., 1993). Like fission yeast Sds22, *S. cerevisiae* Sds22p interacts with $PP1_C$ (Glc7p) as established by multiple criteria (Hisamoto et al., 1995; Hong

Table 1. Primers used in this study

Name	Sequence
KS$^-$	CGAGGTCGACGGTATCG
SDS22Δ	GCCGACGAAGCGTTCTT
SDS22-3	AAATAGATCGATTGACCCG
180	GGGCTCGAGCAAAAGCTCATTTCTGAAGAGGACTTGAATGGAGAACAGAAATTGATAAGTGAGGAAGACC
181	CTGGAATTCAAATCCTCCTCGGAGATTAACTTCTGCTCACCGTTGAGGTCTTCCTCACTTATCAATTTCTG
182	GCCTCTTATATATGTCGCATC
183	GATGCGACATATATAAGAGGCGAGCAAAAGCTCATTTCTG
184	TCATTTCTTGATCAAGATCAGCCATTCAAATCCTCCTCGG
SDS22-PrA-5′	AGAAAACTGACTATGAACTTACCTCCATCCCTACAGAAGATTGATGCGACATATATAAGAGGCGGAGCAGGGGCGGGTGC
SDS22-PrA-3′	TATATATATATATATATGTTTGTGTGTGTATATAAAAAAAAAATCATTTCTTGATCAAGATCAGAGGTCGACGGTATCGATAAG
PrA-GLC7-5′	GAAATGGACACTAGTGCCCACGATGAAGCCGTAGAC
PrA-GLC7-3′	CCAATAATCTATCGATGATATTATCAACGTCAACTGGTTGTGAGCCCTGGAAGTACAGGTTCTCGCTAGCACCCGCTGACGAATTCGCGTCTACTTTCG

Table 2. Yeast strains used in this study

Strain	Genotype*	Source/Reference
AY925	*MAT***a** W303	Kim Arndt
AYS927	*MAT***a** /*MATα* W303	Black et al., 1995
EG1085-10A	*MAT***a** KT1357 *leu2::sds22-6::LEU2*	This study
EG1085-4B	*MAT***a** KT1357 *leu2::sds22-6::LEU2 ipl1-2*	This study
EG1085-12A	*MAT***a** KT1357 *leu2::sds22-6::LEU2 sds22::TRP1*	This study
EG1085-12C	*MAT***a** KT1357 *leu2::sds22-6::LEU2 sds22::TRP1 ipl1-2*	This study
K5043	*MATα* W303*CFIII (CEN3.L.YPH278) URA3 SUP11*	Michaelis et al., 1997
KT1357	*MAT***a** *leu2 his3 ura3-52 trp1*	Bloecher and Tatchell, 2000
KT2066	*MAT***a** /*MATα* KT1357*ura3::GFP-GLC7::URA3/ura3::GFP-GLC7::URA3 sds22::TRP1/ sds22::TRP1 leu2::sds22-6::LEU2/leu2::sds22-6::LEU2*	This study
KT2067	*MAT***a** /*MATα* KT1357*ura3::GFP-GLC7::URA3/ura3::GFP-GLC7::URA3 sds22::TRP1/+ leu2::sds22-6::LEU2/+*	This study
KT2070	*MAT***a** /*MATα* KT1357*ura3::GFP-GLC7::URA3/ura3::GFP-GLC7::URA3*	This study
LKY118	*MAT***a** W303 *glc7::LEU2 trp1-1::*YIplac204-*HA-GLC7*	This study
LKY150	*MAT***a** W303 *glc7::LEU2 trp1-1::*YIplac204-*PrA-GLC7*	This study
LKY168	*MAT***a** W303 *glc7::LEU2 trp1-1::*YIplac204-*HA-GLC7 SDS22-PrA::Sphis5*$^+$	From LKY118 × SAY1230
MPY1000	*MAT***a** W303 *sds22::TRP1 his3::*pRS303-*SDS22*	This study
MPY1001	*MAT***a** W303 *sds22::TRP1 his3::*pRS303-*sds22-6*	This study
MPY1010	*MAT***a** W303 *sds22::TRP1 his3::*pRS303-*SDS22 CFIII (CEN3.L.YPH278) URA3 SUP11*	From MPY1000 × K5043
MPY1020	*MAT***a** W303 *sds22::TRP1 his3::*pRS303-*sds22-5 CFIII (CEN3.L.YPH278) URA3 SUP11*	From SAY1000 × K5043
MPY1030	*MAT***a** W303 *sds22::TRP1 his3::*pRS303-*sds22-6 CFIII (CEN3.L.YPH278) URA3 SUP11*	From MPY1001 × K5043
MPY1165	*MAT***a** W303 *sds22::TRP1 his3::*pRS303-*SDS22 glc7::LEU2* [YCpHA*GLC7*]	This study
MPY1171	*MAT***a** W303 *sds22::TRP1 his3::pRS303-sds22-6 glc7::LEU2* [YCpHA*GLC7*]	This study
PAY701-2	*MAT***a** W303 *glc7::LEU2 trp1*:: YIplac204-*glc7-12*	Paul Andrews
PAY703-1	*MAT***a** W303 *glc7::LEU2 trp1*:: YIplac204-*glc7-5*	Paul Andrews
SAY100	*MAT***a** W303 *sds22::TRP1* [pLMY-SDS22]	This study
SAY102	*MATα* W303*sds22::TRP1* [pLMY-SDS22]	This study
SAY284	*MAT***a** W303 *sds22::TRP1* [YCp6-15]	This study
SAY326	*MAT***a** W303 *sds22::TRP1* [YCp3M*SDS22*]	This study
SAY302	*MATα* W303 *sds22::TRP1 leu2-3,112::*YIp22-5	This study
SAY304	*MATα* W303*sds22::TRP1 leu2-3,112::*YIp22-6	This study
SAY306	*MATα* W303 *sds22::TRP1 leu2-3,112::*YIpLMY	This study
SAY338	*MAT***a** W303 *sds22::TRP1* [YCp6-15,YCpHA*GLC7*]	This study
SAY340	*MAT***a** W303 *sds22::TRP1* [YCp6-15, YCpHA*glc7-12*]	This study
SAY342	*MAT***a** W303 *sds22::TRP1* [YCp3M*SDS22*, YCpHA*GLC7*]	This study
SAY344	*MAT***a** W303 *sds22::TRP1* [YCp3M*SDS22*, YCpHA*glc7-12*]	This study
SAY350	*MAT***a** W303 *sds22::TRP1* [YCp*LEU-SDS22*, YCpHA*GLC7*]	This study
SAY352	*MAT***a** W303 *sds22::TRP1* [YCp*LEU-SDS22*, YCpHA*glc7-12*]	This study
SAY1000	*MAT***a** W303 *sds22::TRP1 his3::pRS303-sds22-5*	This study
SAY1228	*MAT***a** W303 *SDS22-PrA::Sphis5*$^+$	This study
SAY1230	*MAT*α W303 *SDS22-PrA::Sphis5*$^+$	This study
SBY-SS**a**	*MAT***a** W303 *glc7::LEU2* [YCp*GLC7*(*URA3*)]	Andrews and Stark, 2000

*W303 background: *ade2-1 his3-11,15 leu2-3,112 trp1-1 ura3-1 can1-100 ssd1-d2*.

et al., 2000; MacKelvie et al., 1995). Extra copies of *SDS22* suppress the temperature-sensitivity of *glc7-12*, a *GLC7* allele that confers a mitotic arrest phenotype (MacKelvie et al., 1995). Thus, work in both *S. cerevisiae* and *S. pombe* supports a model whereby Sds22p activates mitosis-specific functions of $PP1_C$, and evidence from the latter yeast suggests that, like other PP1 regulatory subunits, Sds22p might act by modifying the substrate specificity of $PP1_C$ (Stone et al., 1993). A human homologue of Sds22p has also been identified (Renouf et al., 1995), but like several of the other nuclear proteins that bind $PP1_C$, human Sds22 appears to act as an inhibitor of $PP1_C$ using the specific substrates tested (Dinischiotu et al., 1997).

In this study, we have generated conditional *sds22* alleles in

Table 3. Plasmids used in this study

Name	Description	Source/Reference
pBS351	pBluescript KS$^-$ carrying *SDS22*	MacKelvie et al., 1995
pLMY-*SDS22*	*URA3 CEN* plasmid carrying *SDS22*	MacKelvie et al., 1995
PNOPPATA-1L	*LEU2 CEN NOP1* promoter::protein A (2 × IgG binding domains)::TEV site::*ADH1* terminator	Lau et al., 2000
pRS303-*SDS22*	pRS303 (Sikorski and Hieter, 1989) carrying a 2.2 kb *Spe*I-*Xho*I fragment encoding *SDS22*	This study
pRS303-*sds22-5*	*sds22-5* version of pRS303-*SDS22*	This study
pRS303-*sds22-6*	*sds22-6* version of pRS303-*SDS22*	This study
p*sds22-6*	pBluescript KS- carrying a 1.1 kb *Spe*I-*Eco*RI fragment from pLMY-*SDS22* joined to the 1.14 kb *Eco*RI-*Hin*dIII fragment from pSHM83	This study
pSHM83	YCpLEU-*SDS22* carrying *sds22-6* allele	This study
pZZ-His5	pBluecript carrying a ZZ tag and *S. pombe his5*$^+$	Rayner and Munro, 1998
YCpHA*GLC7*	YCp50 derivative with HA-tagged *GLC7, HIS3*	Andrews and Stark, 2000
YCpHA*glc7-12*	Version of YCpHA*GLC7*carring the *glc7-12* allele	Andrews and Stark, 2000
YCpLEU-*SDS22*	YCplac111 (*CEN, LEU2*) (Gietz and Sugino, 1988) carrying *SDS22*	This study
YCp3M*SDS22*	Wild-type version of YCp3M*sds22-6*	This study
YCp3M*sds22-6*	YCp6-15	This study
YEp*GLC7*	2.8 kb *Bam*HI-*Hin*dIII fragment carrying *GLC7* in YEplac195 (2μ, *URA3*) (Gietz and Sugino, 1988)	This study
YEpLEU2-*GLC7*	2.8 kb *Bam*HI-*Hin*dIII fragment carrying *GLC7* in YEplac181 (2μ, *LEU2*) (Gietz and Sugino, 1988)	This study
YEp*SDS22*	Blunted 1.35 kb *Bsc*I-*Xho*I fragment of pLMY-*SDS22* inserted into the blunted *Eco*RI-*Pst*I sites of YEplac195 (*CEN, URA3*) (Gietz and Sugino, 1988)	This study
YIp22-5	*sds22-5* version of YIpLMY	This study
YIp22-6	*sds22-6* version of YIpLMY	This study
YIplac204-*glc7-5*	Version of YIplac204-*GLC7* (Andrews and Stark, 2000) carrying the *glc7-5* mutant allele (encoding an F226L substitution)	Paul Andrews
YIplac204-*glc7-12*	Version of YIplac204-*GLC7* (Andrews and Stark, 2000) carrying the *glc7-12* (MacKelvie et al., 1995) mutant allele	Paul Andrews
YIplac204-*HA-GLC7*	YIplac204 (*TRP1*; Gietz and Sugino, 1988) carrying HA-tagged *GLC7* on a 2.5 kb *Hin*dIII-*Msc*I fragment	This study
YIplac204-*PrA-GLC7*	YIplac204 (*TRP1*) (Gietz and Sugino, 1988) carrying PrA-*GLC7*	This study
YIpLMY	YIplac128 (*LEU2*) (Gietz and Sugino, 1988) carrying a 2.2 kb *Spe*I-*Xho*I fragment encoding *SDS22*	This study

order to develop a better understanding of how Sds22p regulates Glc7p function. Surprisingly, we found no evidence of a mitotic arrest phenotype when strains carrying two distinct, temperature-sensitive *sds22* alleles were shifted to the restrictive temperature. However, the mutant strains showed clear evidence of chromosome instability, suggestive of a chromosome segregation defect. Strikingly, the *sds22* mutations led to a rapid loss of nuclear Glc7p localization under restrictive conditions, showing that Sds22p plays a role in maintaining the normal nuclear localization of Glc7p.

Materials and Methods

General methods, strains and plasmids

Basic yeast methods and growth media were as described (Kaiser et al., 1994) and yeast transformation was carried out as described (Gietz et al., 1992). Routine recombinant DNA methodology was performed as described elsewhere (Sambrook et al., 1989). All restriction enzymes were from New England Biolabs (Beverly, MA). Oligonucleotide primers used are summarized in Table 1. When testing for suppression of Ts$^-$ mutations by genes present on high-copy plasmids, cultures of strains grown under selection for the plasmid were diluted to 5×10^5, 5×10^4 and 5×10^3 cells/ml in YPD medium and samples (approximately 5 μl) spotted on YPD agar using a multipronged inoculating manifold (Dan-Kar Corp.). All yeast strains and plasmids used in this study are summarized in Table 2 and Table 3, respectively. To generate SAY100, AY927 was transformed with an *sds22::TRP1* construct and a derivative in which one genomic copy of *SDS22* had been replaced by the knockout was generated and verified as previously described (MacKelvie et al., 1995). After transformation of this strain with pLMY-SDS22, SAY100 was generated following sporulation and tetrad dissection. Chromosome loss was measured using a method developed previously (Spencer et al., 1990) in which loss of a chromosome III fragment carrying the *SUP11* gene was monitored by the red pigment formed upon loss of suppression of the *ade2-101* mutation. Chromosome loss rate per cell division was calculated as described previously (Yoon and Carbon, 1999). FACS analysis was carried out as reported elsewhere (Andrews and Stark, 2000).

Generation of conditional *SDS22* alleles

SDS22 was first inserted as a 1.35 kb *Bsc*I-*Xho*I fragment from pLMY-SDS22 between the *Eco*RI and *Pst*I sites of YCplac111 after both vector and insert had been treated with the Klenow fragment of T4 DNA polymerase to generate blunt ends. The resulting plasmid (YCpLEU-SDS22) was digested with *Pst*I and *Nde*I to remove codons 33-273 of *SDS22*. A PCR fragment encompassing *SDS22* was amplified with primers SDS22Δ KS$^-$ with pBS351 as template, using mutagenic conditions as described previously (Stark, 1998) but with a Mn^{2+} concentration of 0.3 mM. The former primer corresponds to a region ~300 bp downstream of *SDS22*, while the latter primer corresponds to vector sequence upstream of *SDS22* in the template construct. The PCR fragment was digested with *Eco*RI and *Bcl*I, the 1.01 kb central portion was gel purified and then co-transformed with gapped YCpLEU-SDS22 into SAY102. After eviction of pLMY-SDS22 by growth on 5-fluoroorotic acid (5-FOA), 600 transformants were screened for temperature-sensitive growth at 37°C and the *sds22-5* and *sds22-6* alleles thus isolated. The sites of mutational alteration in these alleles were identified by DNA sequence analysis. Strains in which the mutant alleles were integrated at either the *LEU2* or the *HIS3* loci were generated by transformation of SAY100 with derivatives of YIplac128 (Gietz and Sugino, 1988) or pRS303 (Sikorski and Hieter, 1989), respectively, carrying either wild-type *SDS22, sds22-5* or *sds22-6* as a 2.2 kb *Spe*I-*Xho*I fragment inserted into the *Xba*I-*Sal*I interval of the vector. Integration was verified by Southern blot analysis and then strains dependent solely on the integrated copy were obtained following 5-FOA selection (Sikorski and Boeke, 1991).

Sds22p-myc$_3$ and Sds22-6p-myc$_3$

A triple *myc* epitope tag was inserted immediately after the last sense codon of *SDS22* as follows. First, equimolar amounts of primers 180 and 181, which share 25 bp of complementarity at their 3′ ends, were

annealed together by heating at 100°C for 5 minutes followed by slow cooling to room temperature. The 3′ ends were extended at 72°C by addition of dNTPs and Expand™ High-Fidelity Polymerase (Roche), forming a DNA fragment encoding a triple *myc* epitope (*myc*$_3$). After addition of primers 183 and 184, the ~130 bp *myc*$_3$ fragment was amplified by 30 cycles of 1 minute at 95°C, 1 minute at 50°C and 2 minutes at 72°C such that it was flanked by sequences just preceding and just following the *SDS22* stop codon. In a second PCR reaction, the *SDS22* open reading frame was similarly amplified using primers SDS22-3 and 182. The two products were recovered using the High Pure PR product purification kit (Roche) and then fused by mixing equimolar amounts, annealing as described above and amplifying the fusion product using primers Sds22-3 and 184. The product was recovered as above and cleaved with *Nde*I and *Bcl*I to generate a 306-bp fragment corresponding to the C-terminal, *myc*-tagged region of *SDS22*. This fragment was inserted into p*sds22-6* cleaved with the same enzymes, generating a *myc*$_3$-tagged *sds22-6* allele. The tagged gene was verified by DNA sequencing and moved as an *Spe*I-*Hin*dIII fragment into YCplac111 (cut with the *Xba*I-*Hin*dIII) to generate YCp3Msds22-6. A wild-type tagged *SDS22* construct was then generated by replacing the ~800 bp *Pst*I-*Nde*I interval of YCp3Msds22-6 with the corresponding wild-type sequence, generating YCp3MSDS22. Strains dependent on the tagged wild-type or mutant alleles were generated by transformation of SAY100 followed by selection for loss of pLMY-SDS22 using 5-fluoroorotic acid.

Protein A-tagged constructs

A derivative of strain AYS927 in which the genomic copy of *SDS22* was tagged at the 3′ end with protein A was generated as described (Rayner and Munro, 1998), using primers SDS22-PrA-5′ and SDS22-PrA-3′ with pZZ-His5 as template. Following verification by PCR and detection of the tagged protein by western blot analysis, haploid strains in which protein A-tagged Sds22p (Sds22p-PrA) was the sole source of Sds22p function were generated by tetrad analysis.

To generate an integrative plasmid encoding protein A-tagged Glc7p, the HA-tagged *GLC7* construct from YCpHA-*GLC7* was excised as a *Hin*dIII-*Msc*I fragment and cloned between the *Hin*dIII and *Sma*I sites of YIplac204. A small *Spe*I-*Cla*I fragment at the 5′ end of *GLC7* (carrying the HA epitope tag) was removed and replaced with a larger *Spe*I-*Cla*I fragment carrying a protein A tag and TEV protease cleavage site, generating YIplac204-PrA-*GLC7*. This fragment was made by PCR using primers PrA-GLC7-5′ and PrA-GLC7-3′ with pZZ-His5 as template, and was cleaved by *Spe*I and *Cla*I prior to subcloning. The sequence of this fragment was verified by DNA sequencing of the relevant region of the final construct. To generate a strain (LKY150) solely dependent on PrA-Glc7p for Glc7p function, YIplac204-PrA-*GLC7*was integrated into SBY-SS**a** at the *trp1-1* locus followed by selection on 5-FOA to remove YCp-*GLC7*(*URA3*). LKY118 was similarly generated usingYIplac204-HA-*GLC7*. A control strain expressing unfused protein A (from the *NOP1* promoter) was generated by transformation of AY925 with pNOPPATA-1L.

Analysis of Glc7p-Sds22p complexes

To identify proteins complexed with Sds22p, cultures (1.5 l) of strain SAY1228 were grown in YPD medium at 26°C until they reached ~10^7 cells/ml. The cells were harvested by centrifugation and then washed twice with water and finally with 10 ml ice-cold extraction buffer (50 mM Hepes-KOH (pH 7.5), 150 mM KCl, 0.1% Triton X-100, 0.1 mM EDTA, 10% (v/v) glycerol). The cell pellet was resuspended in an equal volume of extraction buffer containing 1× complete protease inhibitors (Roche) and supplemented with an equal volume of acid-washed glass beads (0.4 mm diameter). After 20 cycles of vortexing (30 seconds) and cooling on ice (30 seconds) the cell debris was removed by centrifugation for 10 minutes at 3500 rpm in a Jouan CR/312 centrifuge. The cell pellet was subject to a further 10 cycles of disruption after addition of the same volume of extraction buffer with protease inhibitors and the two resulting supernatants were pooled and spun at 20,000 ***g*** for 20 minutes. Protein A-tagged Sds22p (Sds22-PrA) was recovered from the extract by elution over a column containing 0.75 ml IgG-Sepharose (Amersham Pharmacia Biotech) which had been pre-washed with 20 ml extraction buffer. After washing the column with 10 bed volumes of extraction buffer, the column material was resuspended in 3 ml of extraction buffer without Triton X-100 and glycerol but containing 30 units TEV protease (Life Technologies) and incubated for 1 hour at room temperature. The released material was recovered by elution with extraction buffer (lacking Triton X-100 and glycerol) and examined by SDS-PAGE, with silver staining to visualize the protein bands. For identification of protein bands by mass spectrometry, appropriate fractions of eluate were desalted using CentriPlus (Millipore), concentrated using Microcone protein concentrators (Millipore), alkylated with 4-vinylpyridine and separated by SDS-PAGE using 4-12% Bis-Tris gels (Novex). Gels were stained using Coomassie Brilliant Blue and mass fingerprint analysis carried out as described (Morrice and Powis, 1998). Proteins interacting with PrA-Glc7p were similarly identified using strain LKY150. In each case, strain AY925 transformed with pNOPPATA-1L (expressing the unfused protein A tag) (Lau et al., 2000) was used to control for nonspecific protein binding.

The behaviour of Sds22p-PrA on gel filtration of yeast cell extract (prepared as above from strain SAY1228) was examined using a Superose-200 column calibrated with the following markers (Sigma): apoferritin, α-amylase, alcohol dehydrogenase, bovine serum albumin (BSA). SAY1228 also expressed HA-Glc7p as the sole source of $PP1_C$. Sds22p-PrA was located by western blot analysis and its apparent Stokes radius calculated using a plot of $(-\log K_{AV})^{1/2}$ against published values for the Stokes radii of the marker proteins. The sedimentation of Sds22p-PrA in a 10-40% (v/v) glycerol gradient centrifuged at 60,000 rpm in a Beckman SW60 rotor for 8 hours at 4°C was examined using a similar sample of cell extract from LKY168, with thyroglobulin, catalase, aldolase and BSA as markers (Amersham Pharmacia Biotech). The molecular size of Sds22p-PrA was calculated from its Stokes radius and sedimentation coefficient as previously described (Siegel and Monty, 1966).

Immunoprecipitation of Sds22p-Glc7p complexes and western blot analysis

Cultures of yeast cells (200 ml) were grown at 26°C to a density of 1×10^7 cells/ml in YPD, harvested by centrifugation and washed in an equal volume of water. Cells were collected in a 15 ml centrifuge tube and the pellet supplemented with an equal volume of lysis buffer containing 50 mM Tris-HCL (pH 7.5), 100 mM NaCl, 10 mM $MgCl_2$, 5 mM EDTA, 1 mM DTT, 1% (v/v) Triton X-100, 1× complete protease inhibitors (Roche). Acid-washed glass beads (0.4 mm diameter; 0.7 g per ml) were added and the cells lysed by 20 cycles of vortexing for 30 seconds followed by 30 seconds on ice. Extracts were centrifuged for 5 minutes at 21,000 ***g*** to pellet cell debris and the supernatant removed. The glass beads were washed with one pellet volume of lysis buffer and the supernatants pooled. Protein concentrations were determined using the Bio-Rad protein assay. To make Sds22p-myc$_3$ immunoprecipitates, Protein G-Sepharose beads (Amersham Pharmacia Biotech) were first equilibrated in lysis buffer and 80 μl of a 50% suspension used to pre-clear lysates (containing 2.5 mg protein) at 4°C for 2 hours on a rotary mixer. Purified 9E10 monoclonal antibody (1 μg) was added to the pre-cleared lysate and incubated at 4°C for 2 hours with gentle mixing. The antibody-lysate mix was divided into two equal parts and 20 μl 50% Protein G-Sepharose bead suspension added to each. One was incubated at 4°C for 2 hours while the other was incubated at 30°C, both with gentle mixing as above. The beads were recovered by centrifugation, washed

three times in lysis buffer and then resuspended in 30 μl 2× SDS-PAGE sample buffer and boiled for 2 minutes. Recovered proteins were separated by SDS-PAGE on 10% polyacrylamide gels and Sds22p-myc$_3$ and HA-tagged Glc7p visualized by western blotting with ECL detection using either 9E10 with sheep anti-mouse IgG-HRP conjugate (Amersham Pharmacia Biotech) or mouse anti-HA HRP conjugate (Roche), respectively. Similar procedures were used to compare Sds22p-myc$_3$ and HA-tagged Glc7p levels in total cell extracts using anti-calmodulin antibodies (Stirling et al., 1994) to confirm equivalent protein loading.

Immunofluorescence microscopy

Cells were prepared for immunofluorescence microscopy as described (Ayscough and Drubin, 1998) using the general immunofluorescence protocol, but omitting the methanol and acetone fixing step. High-affinity 3F10 (anti-HA) and 9E10 (anti-myc) antibodies were used at dilutions of 1:100 while both sheep anti-mouse IgG-Cy3 conjugate (Sigma) and goat anti-rat IgG-FITC conjugate (Cappel) secondary antibodies were used at 1:200 dilutions. To visualize DNA, the mounting medium contained 1 mg/ml 4′, 6-diamidino-2-phenylindole dihydrochloride (DAPI). Images were acquired using a Deltavision Restoration microscope (Applied Precision Inc., USA) fitted with a Nikon PlanApo 100× (1.4NA) objective and a Photometrics series 350 cooled CCD camera, taking a Z series encompassing the whole cell. Images were deconvolved and processed using the Deltavision Softworx application on a Silicon Graphics Octane Workstation (Silicon Graphics Inc., USA) and a single optical section presented.

Nuclear localization of Glc7p

To monitor the localization of Glc7p in wild-type and *sds22* mutant strains, a functional GFP-Glc7p construct (Bloecher and Tatchell, 2000) was integrated into the *ura3* locus of strains KT2070 (*SDS22/SDS22*), KT2067 (*SDS22/sds22-6*) and KT2066 (*sds22-6/sds22-6*). The *sds22-6* and *sds22::TRP1* alleles were introduced into KT2066 and KT2067 after backcrossing SAY304 seven times to KT1357. For imaging, cells were grown to mid logarithmic phase in synthetic complete medium, collected by centrifugation and then placed on a microscope slide over a thin agarose slab and under a cover slip, as described elsewhere (Waddle et al., 1996). Cells were observed through a 100× N.A. 1.25 Olympus objective equipped with a Bioptechs objective heater (Butler, PA) and images were collected with a 12-bit Princeton Instruments Micro Max CCD camera, capturing images at 30 minute intervals using 2 second exposures at 6% full intensity. All images for a given strain were normalized in the same way but the normalization was different for each strain. To calculate the ratio of nuclear/cytoplasmic fluorescence at each time point, a minimum of 102 cells in which the focal plane went through the nucleus were quantitated using the IPLab Spectrum software. Individual cells were imaged only once to avoid photobleaching.

Results

Budding yeast Sds22p is a nuclear protein that forms a stable complex with Glc7p.

We modified *SDS22* by addition of a triple myc epitope inserted immediately preceding the stop codon. Triple myc-tagged Sds22p (Sds22p-myc$_3$) was fully functional as judged from its ability to support normal growth when present as the sole source of Sds22p. Using such a strain, Sds22p-myc$_3$ was found to be mainly localized to the nucleus (Fig. 1). Although Sds22p largely co-localized with nuclear Glc7p, in some cells Sds22p appeared to be located within a slightly more restricted region of the nucleus than Glc7p, and most cells contained at least some regions where Sds22p did not overlap with Glc7p. We also tagged Sds22p with green fluorescent protein (GFP) and obtained similar results, although the signal obtained was rather weak (not shown). Thus like its fission yeast homologue, Sds22p is largely confined to the nucleus. In view of its potential role in targeting Glc7p to other cellular components, we adopted an affinity isolation approach to identify other polypeptides with which Sds22p could interact. Sds22p was tagged with Protein A at its C-terminus (Sds22p-PrA) and a strain in which Sds22p-PrA was the sole source of Sds22p was generated. Sds22p-PrA was affinity isolated on IgG Sepharose and proteins that co-purified were recovered following cleavage of the fusion protein by TEV protease at a site immediately preceding the Protein A tag. However, comparison with a control strain expressing unfused Protein A showed that only two specific bands were present in the Sds22p-Protein A TEV eluate, and mass fingerprint analysis revealed that these were Sds22p and Glc7p (Fig. 2A). By comparison, when a similar approach was used to examine Glc7p-associated proteins, several polypeptides could be specifically isolated in complexes with Protein A-tagged Glc7p, although Sds22p represented one of the more abundant Glc7p-associated proteins (Fig. 2B). Catalytic activity of the Glc7p polypeptide is not required for its interaction with Sds22p since Sds22p could still form a complex with Glc7p containing an inactivating mutation (H124A) at the catalytic site (not shown).

To determine what proportion of Sds22p was complexed with Glc7p, HA-tagged Glc7p (HA-Glc7p) was immunodepleted from extracts and the behaviour of Sds22p-PrA examined. Fig. 2C shows that near complete immunodepletion of HA-Glc7p concurrently removed most of the Sds22p-PrA from the extract, demonstrating that the majority of Sds22p-PrA present must be complexed with Glc7p. When Sds22p-PrA was examined by gel filtration, it eluted as a single peak with a Stokes radius of ~45 Å, which

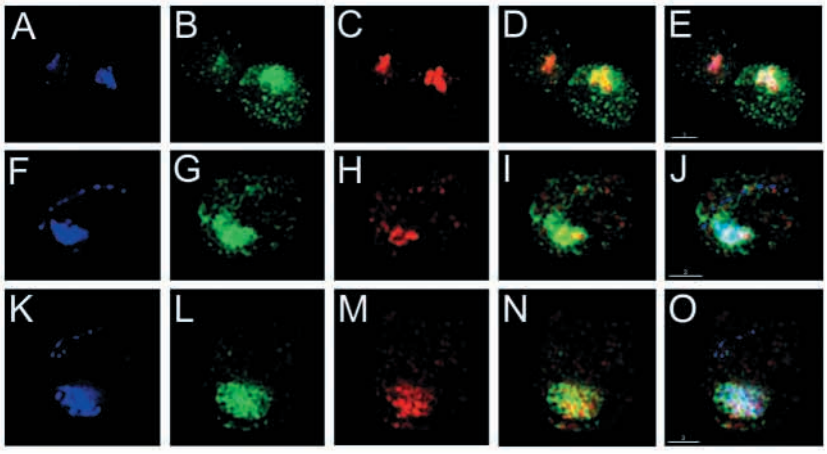

Fig. 1. Nuclear localization of Sds22p. Sds22p-myc$_3$ and HA-Glc7p were localized by indirect immunofluorescence microscopy using strain SAY342 and data presented for three representative cells. A,F,K, DAPI fluorescence; B,G,L, HA-Glc7p; C,H,M, Sds22p-myc$_3$; D,I,N, merged HA-Glc7p/Sds22p-myc$_3$; E,J,O, merged DAPI/HA-Glc7p/Sds22p-myc$_3$. Bar, 2 μm.

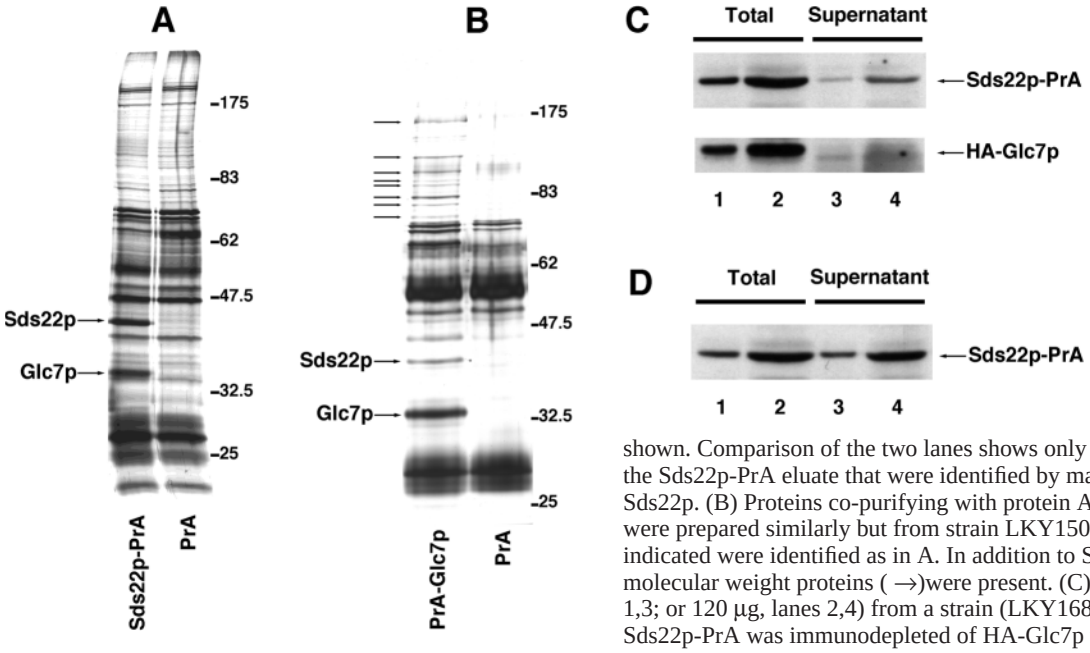

Fig. 2. The Sds22p-Glc7p complex. (A) Proteins bound by protein A-tagged Sds22p (Sds22p-PrA) were recovered from extract of strain SAY1230 after affinity isolation on IgG-Sepharose followed by elution of Sds22p protein complexes with TEV protease, which cleaves between Sds22p and the protein A tag. Proteins present in the eluate when control extracts in which the protein A tag alone (PrA) was expressed are also shown. Comparison of the two lanes shows only two major bands specific to the Sds22p-PrA eluate that were identified by mass spectrometry as Glc7p and Sds22p. (B) Proteins co-purifying with protein A tagged Glc7p (PrA-Glc7p) were prepared similarly but from strain LKY150 and the two major bands indicated were identified as in A. In addition to Sds22p, several other higher molecular weight proteins (→)were present. (C) Protein extract (30 μg, lanes 1,3; or 120 μg, lanes 2,4) from a strain (LKY168) expressing HA-Glc7p and Sds22p-PrA was immunodepleted of HA-Glc7p using anti-HA antibodies and the amount of HA-Glc7p or Sds22p-PrA remaining after immunodepletion (supernatant) compared with the initial level (total) by western blot analysis. (D) Control experiment using a strain with untagged Glc7p (SAY1228), confirming that Sds22p-PrA is not depleted by the anti-HA antibodies used in (C).

overlapped with fractions containing HA-Glc7p, although HA-Glc7p was also present in the void volume and in fractions that eluted later than Sds22p-PrA, demonstrating that not all HA-Glc7p was bound to Sds22p-PrA (not shown). When Sds22p-PrA was analysed by glycerol density gradient ultracentrifugation, it sedimented as a single peak of ~5S which overlapped with the sedimentation profile of HA-Glc7p (not shown). The method of Siegel and Monty (Siegel and Monty, 1966) yielded an estimated M_r of ~93,000 based on these data. This estimate is consistent both with the expected size of a 1:1 Sds22p-PrA–HA-Glc7p complex (M_r 91,759) and with the failure to identify any other Sds22p-interacting proteins at stoichiometric levels. Thus, like Hong et al. (Hong et al., 2000), we conclude that Sds22p forms a stable complex with Glc7p and that this complex is unlikely to contain any other components. This differs from results obtained in HeLa cell extracts, where human Sds22p was found in a much larger complex of approximately 260 kDa (Dinischiotu et al., 1997).

Conditional *sds22* alleles

To gain greater insight into the role of Sds22p, we next generated temperature-sensitive *sds22* alleles by random PCR-mediated mutagenesis. Of several such alleles isolated we chose to characterize two in particular. *sds22-5* was found to carry four point mutations leading to four amino acid replacements in the protein (T25A, Q28R, L73P, F285S), while *sds22-6* encodes two missense mutations (I54T, I193T) together with a silent mutation in codon 51. The L73P and F285S mutations in *sds22-5* and the I193T mutation in *sds22-6* represent nonconservative changes to key hydrophobic residues located in leucine-rich repeats (LRRs) 1 and 10 (*sds22-5*) and in LRR 6 (*sds22-6*). Both alleles were found to be recessive (not shown). Strains dependent on either plasmid-borne or integrated copies of *sds22-5* were unable to grow at 32°C or higher, while the equivalent *sds22-6* strains grew up to 35°C. In the presence of nocodazole, strains containing either the *sds22-5* or *sds22-6* allele arrested with a large-budded morphology at the same concentration required to provoke an equivalent arrest in the *SDS22* control strain, and this arrest was maintained for 3 hours when the nocodazole-arrested cultures were shifted to 37°C (not shown). Thus, continued Sds22p function is not required for maintenance of a mitotic checkpoint arrest. Although in W303 strains high-copy *GLC7* is unable to compensate for complete loss of *SDS22* function (not shown), the restrictive temperature of each *sds22* mutant was raised significantly by high-copy *GLC7* (Fig. 3; and data not shown), suggesting that elevated levels of Glc7p can in part compensate for loss of Sds22p function. High-copy *SDS22* was similarly able to raise the restrictive temperature of the *glc7* alleles *glc7-5* and *glc7-12* (Fig. 3). Taken together, these genetic data support a model whereby Sds22p and Glc7p function in an interdependent manner.

Since Glc7p is required for kinetochore function and chromosome stability (Sassoon et al., 1999), we examined chromosome loss rates in the *sds22* mutant strains using a standard colony-sectoring assay. Both *sds22-5* and *sds22-6* conferred a marked chromosome loss phenotype at higher growth temperatures, with the *sds22-6* allele showing the greatest defect in chromosome stability (Table 4): at 32°C, which is more than 3°C below the temperature at which *sds22-6* strains fail to grow, the chromosome loss frequency per cell division was elevated around 30-fold compared to wild-type strains. Thus like the *glc7-10* mutant (Sassoon et al., 1999), the Ts$^-$ *sds22* mutants show a profound chromosome loss phenotype at higher growth temperatures. However, unlike *glc7-10* and *glc7-129* $PP1_C$ mutations (Bloecher and Tatchell, 1999; Sassoon et al., 1999), neither *sds22-5* nor *sds22-6* conferred a distinct mitotic arrest phenotype at 37°C: after

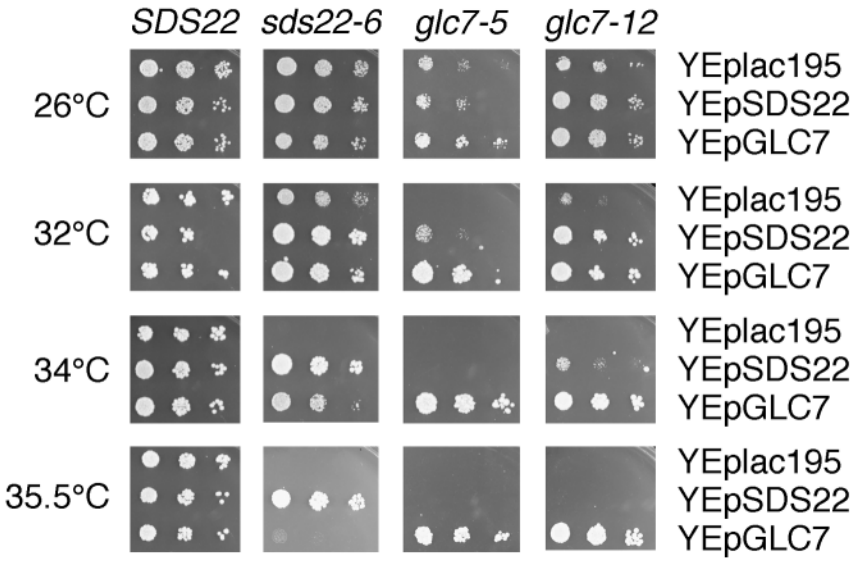

Fig. 3. Reciprocal genetic interactions between *SDS22* and *GLC7*. Tenfold serial dilutions of wild-type, *sds22-6*, *glc7-5* and *glc7-12* strains transformed with empty vector (YEplac195) or high-copy YEplac195 constructs carrying *SDS22* or *GLC7* were plated on YPD agar at different growth temperatures. Partial suppression of *sds22-6* by high-copy *GLC7* and of both *glc7* alleles by high-copy *SDS22* can be seen by growth of the appropriate strains at normally restrictive temperatures.

shifting asynchronous cultures of the mutants to the nonpermissive conditions, little change in the proportion of budded cells could be detected but proliferation ceased within 1-2 generations (not shown). Fig. 4 shows that when cells synchronised in G1 with mating pheromone were released at the restrictive temperature, both *sds22* mutant and wild-type cells initiated budding and DNA replication, although both events were slightly delayed in the mutants. Again, however, no homogeneous arrest phenotype could be observed. In contrast to the *glc7-10* and *glc7-129* $PP1_C$ mutations, the defect in *sds22* mutants that confers chromosome instability does not apparently activate the mitotic checkpoint. This is in contrast to *S. pombe* cells carrying a temperature-sensitive *sds22* allele that arrested in mid-mitosis (Stone et al., 1993).

One way in which *sds22* mutations might exert their effect would be destabilization of the mutant protein. We therefore generated a strain in which a triple myc-tagged copy of *sds22-6* was the sole source of Sds22p and examined Sds22-myc_3 protein levels by western blot analysis following transfer of the strain to 37°C. This showed that the steady-state protein level remained essentially unchanged for at least 6 hours at the restrictive conditions (Fig. 5). Similarly, we found that levels of Glc7p were essentially unchanged in the *sds22-6* mutant strain at 37°C over a similar time course (Fig. 5). Thus loss of

Table 4. Chromosome loss frequency of *sds22* mutant strains

Strain	Growth temperature (°C)	Chromosome loss per division ($\times 10^4$)*
MPY1010 (*SDS22*)	26	3.00
	29	3.23
	32	6.55
MPY1020 (*sds22-5*)	26	7.43
	29	36.2
MPY1030 (*sds22-6*)	26	17.7
	29	25.8
	32	186

*Loss rate per cell division=number of half-sectored colonies/(total colonies-red colonies), where a half-sectored colony is defined as one that contained a white sector occupying no more than half the colony.

Sds22p function conferred by the *sds22-6* allele cannot be explained by instability of either Sds22p or Glc7p at the restrictive temperature. We therefore next tested by co-immunoprecipitation whether the formation of the Sds22p-Glc7p complex was affected by *sds22* mutations. Extracts were made from wild-type or *sds22-6* mutant strains grown under permissive conditions at 26°C and Sds22p immunoprecipitations carried out either at 4°C or 30°C. Although the recovery of Sds22p-myc_3 by immunoprecipitation was lower from the *sds22-6* mutant despite similar overall levels of the protein in the extracts, HA-Glc7p co-precipitated with both wild-type and mutant Sds22p-myc_3 at 4°C (Fig. 6, lanes 3,5). By comparison, when immunoprecipitation was carried out at 30°C, no detectable HA-Glc7p was present in the precipitates (Fig. 6, compare lanes 3 and 5). We also examined whether the *glc7-12* mutation affected formation of the Sds22p-Glc7p complex, but since the level of the HA-tagged mutant Glc7p in the extracts was lower it is difficult to assess whether its reduced recovery in Sds22p immunoprecipitates indicates reduced interaction with Sds22p (Fig. 6, lanes 3,4). However, the Sds22p-Glc7p interaction was not rendered noticeably temperature-sensitive in vitro by the *glc7-12* mutation (Fig. 6, lane 4), in contrast to the effect of *sds22-6.* We conclude therefore that the *sds22-6* mutations affect the interaction of the mutant protein with Glc7p at higher temperatures, consistent with the in vivo temperature-sensitivity of the *sds22-6* mutant strain. The amount of Sds22p-Glc7p complex recovered at 4°C when both proteins were mutated was lower than when extracts contained just one mutant polypeptide (Fig. 6, lane 6). However, since the *glc7-12* mutation reduced the overall level of HA-Glc7p and the immune precipitates from the *sds22-6* strain contained lower levels of Sds22p, the two mutations probably do not confer an additive defect in Sds22p-Glc7p complex formation. This is consistent with our finding that there is no additional growth defect seen when *sds22-6* and *glc7-12* are combined (not shown).

Suppression of *ipl1-2* by *sds22-6*

Recent work has revealed that both histone H3 and the kinetochore protein Ndc10p are likely to be substrates of nuclear PP1. The Ipl1p protein kinase can phosphorylate each of these proteins and both genetic and biochemical approaches have shown that PP1 opposes the action of the Ipl1p kinase in regulating their phosphorylation state (Biggins et al., 1999; Hsu et al., 2000; Sassoon et al., 1999). For example, certain *glc7* loss-

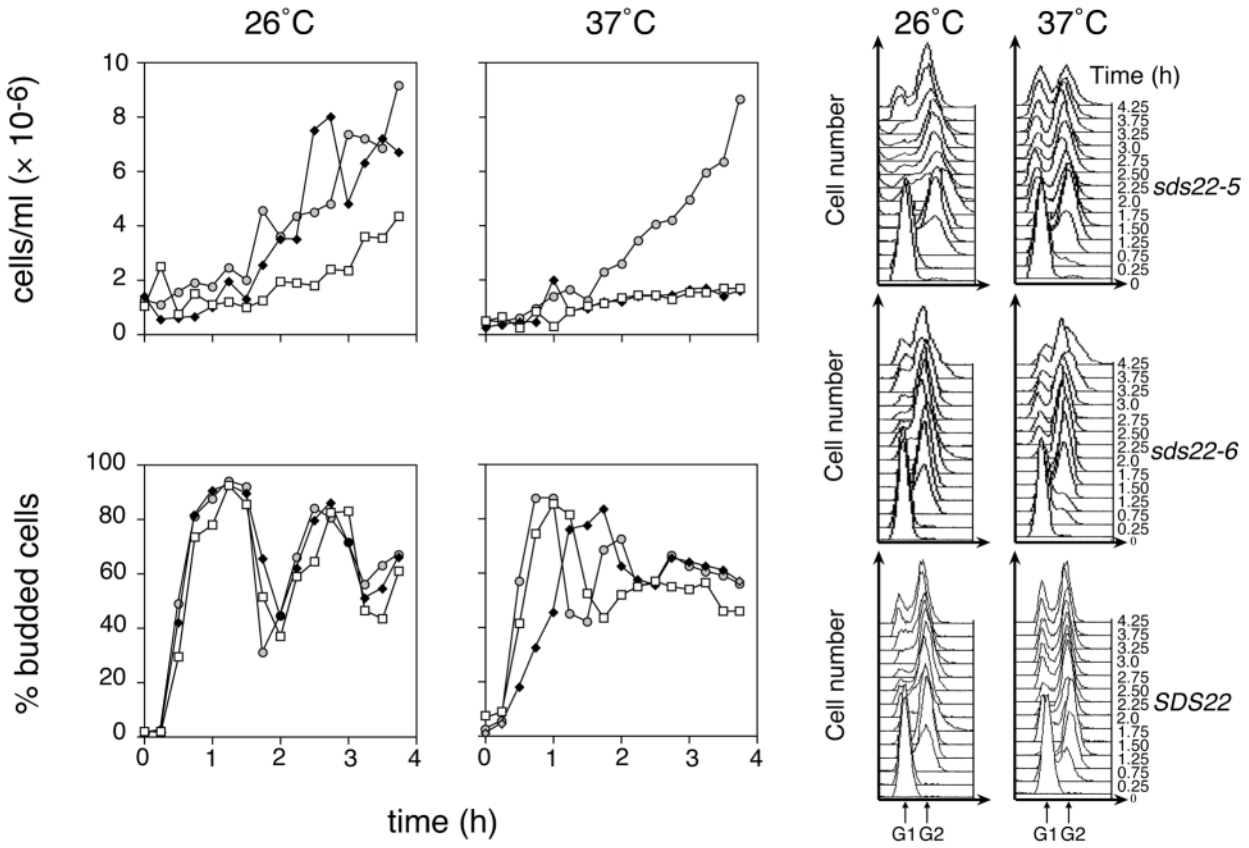

Fig. 4. Release of *sds22* Ts⁻ mutants from alpha-factor arrest. Wild-type, *sds22-5* and *sds22-6* cells were synchronized in G1 using alpha-factor and released at either 26°C or 37°C. Cell density and % budded cells were monitored and the DNA content measured by FACS analysis. At 37°C the mutant cells budded and replicated their DNA, but proliferation ceased after an approximately twofold increase in cell density. ○, wild-type (SAY306);□, *sds22-5* (SAY302); ◆, *sds22-6* (SAY304).

of-function mutants show allele-specific hyperphosphorylation of histone H3 on serine-10, while the *ipl1-2* mutant shows greatly reduced histone H3 serine-10 phosphorylation in vivo. Ipl1p kinase can also phosphorylate histone H3 at this position in vitro. In keeping with the model that Ipl1p kinase and PP1 oppose each other in regulating the phosphorylation state of proteins, *glc7-127* suppressed the temperature-sensitivity of the *ipl1-2* mutation in an allele-specific manner (Hsu et al., 2000). Similarly, *glc7-10*, a PP1 loss of function mutant which is defective in Ndc10p dephosphorylation (Sassoon et al., 1999), and *ipl1-321*, a mutant which lacks a protein kinase activity required for inactivation of kinetochore function in an in vitro assay (Biggins et al., 1999), show mutual suppression (N. Rachidi and M.J.R.S., unpublished). We therefore examined the effect of combining *sds22-6* with *ipl1-2*. If *sds22-6* leads to reduced PP1 activity in vivo then a clear prediction would be that it should relieve the Ts⁻ defect associated with *ipl1-2*. Fig. 7 shows that while the *ipl1-2* strain was unable to grow at 34°C, when combined with *sds22-6* it grew just as well as the *sds22-6 IPL1* control strain and almost as well as a wild-type strain. Thus, like *glc7-127* (Hsu et al., 2000), *sds22-6* suppresses the temperature-sensitivity of the *ipl2-1* mutant. This result is consistent with the notion that the *sds22-6* mutation causes reduced nuclear PP1 function, thereby compensating for the reduced kinase activity in the *ipl1-2* mutant. However, the double *ipl1-2 sds22-6* strain remained unable to grow at 37°C, perhaps either because suppression requires some residual Ipl1p function or because there is incomplete overlap between the cellular targets of the two proteins.

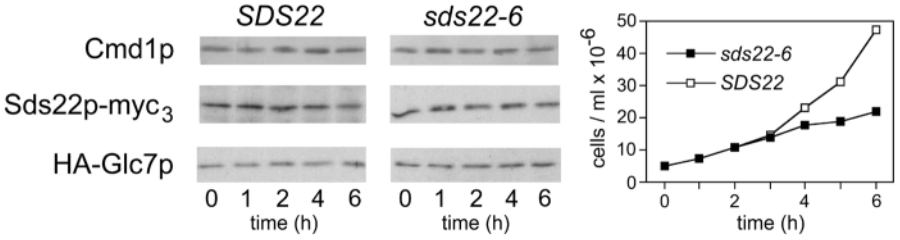

Fig. 5. Stability of Sds22p and Glc7p in the *sds22-6* mutant. Strains solely dependent on myc epitope-tagged wild-type (Sds22p-myc$_3$: SAY326) or mutant (Sds22-6p-myc$_3$: SAY284) Sds22p or wild-type (MPY1165) and *sds22-6* (MPY1171) strains expressing HA epitope-tagged Glc7p (HA-Glc7p) were shifted to 37°C and the stability of either protein monitored by western blot analysis over 6 hours. The level of calmodulin (Cmd1p) is shown to demonstrate equivalent loading of each lane and the growth curve indicates cell density at each time point.

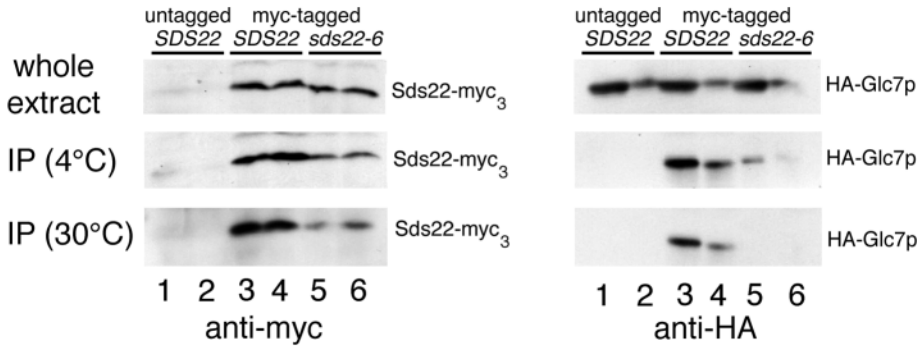

Fig. 6. Effect of *sds22-6* on the Sds22p-Glc7p complex. Strains dependent on untagged Sds22p (SAY350, SAY352; lanes 1,2) or myc epitope-tagged wild-type (Sds22p-myc$_3$: SAY342, SAY344; lanes 3,4) or mutant (Sds22-6p-myc$_3$: SAY338, SAY340; lanes 5,6) Sds22p were transformed with plasmids encoding either HA-Glc7p (lanes 1,3,5) or the equivalent HA-tagged *glc7-12* allele (lanes 2,4,6). Cells were grown at 26°C and myc-tagged Sds22p recovered from extracts by immunoprecipitation after incubation at either 4°C or 30°C. The Sds22p recovered and the amount of co-precipitable Glc7p were visualized by western blot analysis with either anti-myc (left panel) or anti-HA (right panel) antibodies.

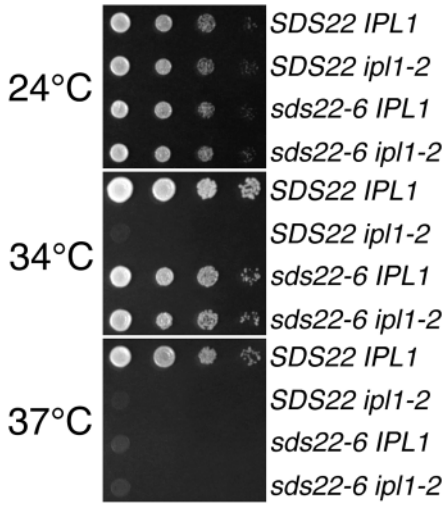

Fig. 7. Suppression of the *ipl1-2* temperature-sensitive phenotype by *sds22-6*. Tenfold serial dilutions of wild-type (EG1085-10A), *ipl1-2* (EG1085-4B) *sds22-6* (EG1085-12A) and *ipl1-2 sds22-6* (EG1085-12C) were plated onto YPD agar and incubated for 2 days at the indicated growth temperatures.

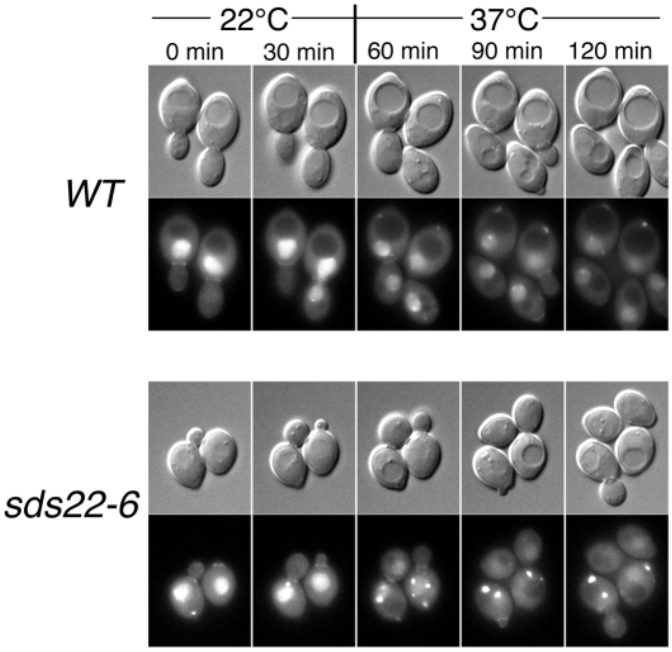

Fig. 8. Glc7p localization is affected in the *sds22-6* mutant. Diploid *SDS22/SDS22* (KT2070), *sds22-6/sds22-6* (KT2066) and *SDS22/sds22-6* (KT2067) cells expressing GFP-Glc7p were grown at 22°C and then shifted to 37°C. The effect of the temperature shift on wild-type and mutant cells is presented for a representative field, showing DIC and GFP fluorescence images for each time point.

Normal nuclear localization of PP1 requires functional Sds22p

The effect on Glc7p localization of shifting *sds22-6* mutant cells to 37°C was next examined using a GFP-Glc7p fusion. In control strains, the nuclear localization of GFP-Glc7p was essentially unaffected by shifting cells to 37°C. However, in the *sds22-6* mutant the relatively uniform nuclear GFP-Glc7p fluorescence in the majority of cells relocalized to a small number of bright foci after as little as 30 minutes (Fig. 8), some but not all of which appeared to be located within the nucleus. To quantitate nuclear levels of GFP-Glc7p, the fluorescence intensity of nuclear and cytoplasmic GFP-Glc7p was measured in over 100 cells at each time point and the nuclear/cytoplasmic ratio was estimated. Table 5 shows that in the *sds22-6* mutant the relative nuclear fluorescence was significantly decreased at 37°C compared with the wild-type. Given that the overall level of Glc7p remained essentially constant after shift to 37°C (Fig. 5B), these data suggest that the *sds22-6* mutation affects the localization of Glc7p under restrictive conditions: overall levels within the nucleus are reduced and, rather than being present throughout the nucleus, it is relocalized into a small number of foci.

Discussion

The Sds22p-Glc7p complex

In this work we have used a variety of biochemical and genetic approaches to address the cellular function of *S. cerevisiae* Sds22p, a putative regulator of protein phosphatase 1 (PP1). One aim was to identify novel Sds22p-interacting proteins as a means of understanding Sds22p function. However, Glc7p was the only protein that could be specifically affinity isolated using protein A-tagged Sds22p. By contrast, Sds22p and a number of as yet uncharacterized proteins could be specifically isolated in complexes with protein A-tagged Glc7p. Furthermore, the majority of Sds22p appears to be bound to Glc7p (Fig. 2C), consistent with their similar patterns of localization within the nucleus. While we cannot rule out the existence of transient interactions between Sds22p and other

Table 5. Effect of *sds22-6* on the nuclear/cytoplasmic ratio of Glc7p

Strain	Temperature/time	Nuclear fluorescence*	Cytoplasmic fluorescence*	Nuclear/cytoplasmic ratio
sds22-6/sds22-6	22°C	475±62	233±36	2.06±0.29
(KT2066)	37°C/30 min	299±42	185±30	1.62±0.25
	37°C/60 min	281±42	185±26	1.53±0.18
	37°C/90 min	250±34	174±27	1.46±0.17
sds22-6/SDS22	22°C	494±66	206±35	2.43±0.34
(KT2067)	37°C/30 min	319±48	150±24	2.15±0.29
	37°C/60 min	271±53	134±24	2.04±0.27
	37°C/90 min	226±30	114±15	2.01±0.28
SDS22/SDS22	22°C	459±51	197±28	2.36±0.28
(KT2070)	37°C/30 min	373±49	186±30	2.04±0.29
	37°C/60 min	377±45	181±26	2.11±0.30
	37°C/90 min	371±52	180±30	2.09±0.30

*Calculated on samples of at least 102 cells in which the focal plane passed through the nucleus, imaging each cell only once.

proteins that would not have been detected by this approach, for example any potential substrates of an Sds22p-Glc7p complex, the evidence strongly points to the absence of any other proteins stably and stoichiometrically associated with the Sds22p-Glc7p complex. This is fully consistent with the apparent molecular size of Sds22p in cell extracts determined from two different biophysical parameters and which strongly suggests a 1:1 stoichiometry. In vitro, the mutant *sds22-6* product is profoundly defective in its ability to bind Glc7p at high temperatures. This suggests that the ability to form the Sds22p-Glc7p complex is critical and is consistent with the reciprocal high-copy suppression data shown in Fig. 3. $PP1_C$ interacts with many of its regulatory subunits via a -V/IXF- $PP1_C$ binding motif in the latter, which interacts with a cleft on the opposite face of the phosphatase to the catalytic site (Egloff et al., 1997). Since Sds22p lacks such a sequence, its mode of interaction with $PP1_C$ must be distinct, consistent with the finding that Glc7p carrying mutations in the -V/IXF- binding cleft interacts normally with Sds22p (Wu and Tatchell, 2001). It would therefore be interesting to determine the structure of the Sds22-$PP1_C$ complex to uncover the molecular basis of the Sds22p-Glc7p interaction.

Localization of Sds22p

As previously found for its human and fission yeast homologues, *S. cerevisiae* Sds22p is a nuclear protein despite the absence of any clearly defined monopartite (Kalderon et al., 1984) or bipartite (Robbins et al., 1991) nuclear localization sequence (NLS). Although a 39 kDa polypeptide such as Sds22p could potentially gain entry to the nucleus without the aid of a specific import signal, we think this is unlikely in the case of Sds22p, which is largely composed of LRRs and is therefore expected to be non-globular and rather asymmetric (Kobe and Deisenhofer, 1994). In this case, Sds22p may either contain a novel signal for nuclear import, or alternatively it could be imported as a complex with another protein such as Glc7p. Although Glc7p has an excellent candidate monopartite NLS (RKKK) at its extreme C-terminus, recent work suggests that this region is not essential either for Glc7p nuclear localization or function (Hong et al., 2000). Furthermore, mutant Sds22 proteins in fission yeast that failed to bind $PP1_C$ could nonetheless localize to the nucleus, while other variants which were excluded from the nucleus could still bind $PP1_C$ (Stone et al., 1993), strengthening the idea that $PP1_C$ binding and nuclear import are not obligatorily linked. Additional examples of nuclear LRR proteins that also apparently lack a classical NLS include *Drosophila* LRR47 (Buchanan et al., 1998) and the human splicing factor U2A' (Sillekens et al., 1989), although other LRR proteins such as CIITA (a transactivator of human MHC class II genes) (Hake et al., 2000), contain potential NLSs as well as LRRs. Mutations in the LRR region of CIITA specifically affect its nuclear localization (Hake et al., 2000). It is therefore conceivable that LRRs constitute a novel determinant of nuclear import, although this could be due to their role as mediators of protein-protein interaction rather than because they contain an intrinsic nuclear import signal. In fission yeast Sds22, mutational analysis revealed that C-terminal truncation or point mutations in LRRs 5 or 9 led to nuclear exclusion of the mutant proteins and loss of function, although mutations in some of the other LRRs failed to affect nuclear localization (Stone et al., 1993).

Sds22p function

The cellular role of Sds22p is clearly a critical question and at least two types of model can be proposed for how the Sds22p-Glc7p complex might influence $PP1_C$ activity. One possibility is that Sds22p activates Glc7p function towards key nuclear $PP1_C$ substrates that are required for chromosome stability and other functions. This is supported by the reciprocal, high-copy suppression by each gene of recessive mutations in the other, and by the finding that *sds22-6* mimics *glc7* mutations in partially suppressing *ipl1-2* temperature-sensitivity (Hsu et al., 2000). This suggests that Sds22p and Glc7p function together in a positive sense to create a nuclear PP1 activity. Furthermore, although fission yeast Sds22 immunoprecipitates lacked the phosphorylase phosphatase activity shown by $PP1_C$ alone, they contained a histone H1 phosphatase activity (Stone et al., 1993), supporting a model whereby the Sds22-$PP1_C$ complex can be active as a phosphatase, at least against certain substrates. However, when Sds22p function is lost, the normally uniform nuclear localization of Glc7p is dramatically changed such that the overall level of nuclear PP1 is reduced and the remaining PP1 becomes localized in a small number of foci. Since the interaction of Glc7p with the mutant *sds22-6* polypeptide is itself temperature-sensitive, this suggests that

Sds22p binding is required to maintain proper nuclear localization of Glc7p. A second possibility is therefore that Sds22p plays a chaperone-like role for nuclear Glc7p, preventing aggregation of the free $PP1_C$ subunit and/or helping to retain it in the nucleus, but not necessarily directing it towards specific substrates. This model would predict that the *sds22* mutations might affect a wider range of nuclear $PP1_C$ functions.

In addition to the dramatic effect of *sds22-6* on nuclear localization of Glc7p, both *sds22* alleles described here confer a profound chromosome loss phenotype at higher growth temperatures. If reflected uniformly across all 16 chromosomes, the high rates of loss seen in *sds22-6* at 32°C would suggest that only ~75% of cells would inherit a complete genome at each cell division. High-copy *GLC7* also promotes chromosome instability (Francisco et al., 1994) and exacerbates the chromosome loss defect in the *sds22* mutants despite partially suppressing their growth defect (M.W.P. and M.J.R.S., unpublished). Thus the lethality of the *sds22* mutants is unlikely to result from chromosome loss per se. A number of *glc7* alleles including *glc7-10* (Sassoon et al., 1999), *glc7-129* (Bloecher and Tatchell, 1999) and *glc7-12* (MacKelvie et al., 1995) A. Engles and M.J.R.S., unpublished) confer a mitotic arrest phenotype due to mitotic checkpoint activation. Such mutants show an in vitro defect in microtubule binding by kinetochores (Sassoon et al., 1999) (I. Sassoon et al., unpublished) that if representative of the in vivo situation would be sufficient to account for the observed checkpoint activation This is in contrast to the budding yeast *sds22* mutants described in this work that do not arrest in mitosis despite showing severe chromosome instability at higher growth temperatures. Conversely, the conditional fission yeast *sds22* mutant described by Stone et al. (Stone et al., 1993) arrested homogeneously in mitosis, although it is not known whether this synchronous arrest is checkpoint-dependent. If Sds22p is required generally for nuclear $PP1_C$ function then it is perhaps surprising that our *sds22* mutants do not also activate the checkpoint. However, Glc7p most likely has multiple nuclear roles that do not all result in checkpoint activation. For example, some *glc7* mutants that clearly suppress the temperature-sensitivity of *ipl1-2* and raise the phosphorylation level of histone H3 on ser-10 (*glc7-127*), don't by themselves activate the mitotic checkpoint. Conversely, *glc7-129* mutants lacking the Mad/Bub checkpoint are still delayed at the end of the cell cycle, pointing to an additional defect late in mitosis or during cytokinesis. We have also observed synthetic lethality between *glc7-129* and several genes encoding microtubule motors (A.B. and K.T., unpublished) that point to a cell cycle role separate from microtubule binding at the kinetochore. Perhaps either the *sds22* mutants show chromosome loss for some reason other than faulty kinetochore regulation that does not lead to checkpoint activation or, alternatively, the checkpoint-dependent arrest expected to ensue from the type of kinetochore defect seen in the above *glc7* mutants is masked due to defects in multiple Glc7p nuclear functions.

We thank Kim Nasmyth for providing various yeast strains, Kim Arndt for the HA-tagged *GLC7* construct and Paul Andrews for useful comments and suggestions. We gratefully acknowledge the support of the Wellcome Trust (project grant 046956 to M.J.R.S.) and the National Institutes of Health (NIH grant GM47789 to K.T.).

References

Ajuh, P. M., Browne, G. J., Hawkes, N. A., Cohen, P. T., Roberts, S. G. and Lamond, A. I. (2000). Association of a protein phosphatase 1 activity with the human factor C1 (HCF) complex. *Nucleic Acids Res.* **28**, 678-686.

Alessi, D., MacDougall, L. K., Sola, M. M., Ikebe, M. and Cohen, P. (1992). The control of protein phosphatase 1 by targetting subunits. The major myosin phosphatase in avian smooth muscle is a novel form of protein phosphatase 1. *Eur. J. Biochem.* **210**, 1023-1035.

Allen, P. B., Kwon, Y. G., Nairn, A. C. and Greengard, P. (1998). Isolation and characterization of PNUTS, a putative protein phosphatase 1 nuclear targeting subunit. *J. Biol. Chem.* **273**, 4089-4095.

Andrews, P. D. and Stark, M. J. R. (2000). Type 1 protein phosphatase is required for maintenance of cell wall integrity, morphogenesis and cell cycle progression in *Saccharomyces cerevisiae*. *J. Cell Sci.* **113**, 507-520.

Ayscough, K. R. and Drubin, D. G. (1998). Immunofluorescence microscopy of yeast cells. In *Cell Biology: A Laboratory Handbook* (Vol. 2), pp. 477-485. Academic Press.

Bailis, J. M. and Roeder, G. S. (2000). Pachytene exit controlled by reversal of Mek1-dependent phosphorylation. *Cell* **101**, 211-221.

Biggins, S., Severin, F. F., Bhalla, N., Sassoon, I., Hyman, A. A. and Murray, A. W. (1999). The conserved protein kinase Ipl1 regulates microtubule binding to kinetochores in budding yeast. *Genes Dev.* **13**, 532-544.

Black, S., Andrews, P. D., Sneddon, A. A. and Stark, M. J. R. (1995). A regulated *MET3-GLC7* gene fusion provides evidence of a mitotic role for *Saccharomyces cerevisiae* protein phosphatase 1. *Yeast* **11**, 747-759.

Bloecher, A. and Tatchell, K. (1999). Defects in *Saccharomyces cerevisiae* protein phosphatase type I activate the spindle/kinetochore checkpoint. *Genes Dev.* **13**, 517-522.

Bloecher, A. and Tatchell, K. (2000). Dynamic localization of protein phosphatase type 1 in the mitotic cell cycle of *Saccharomyces cerevisiae*. *J. Cell. Biol.* **149**, 125-140.

Bollen, M. (2001). Combinatorial control of protein phosphatase-1. *Trends Biochem. Sci.* **26**, 426-431.

Buchanan, S. G., Dornan, S. and Gay, N. J. (1998). Promoter sequence and expression of the leucine-rich repeat gene LRR47: evidence for cytoplasmic and nuclear localization in *Drosophila* embryos and cells. *Gene* **211**, 235-244.

Dinischiotu, A., Beullens, M., Stalmans, W. and Bollen, M. (1997). Identification of sds22 as an inhibitory subunit of protein phosphatase 1 in rat liver nuclei. *FEBS Lett.* **402**, 141-144.

Doherty, M. J., Moorhead, G., Morrice, N., Cohen, P. and Cohen, P. T. (1995). Amino acid sequence and expression of the hepatic glycogen-binding (G_L)- subunit of protein phosphatase 1. *FEBS Lett.* **375**, 294-298.

Egloff, M. P., Johnson, D. F., Moorhead, G., Cohen, P. T., Cohen, P. and Barford, D. (1997). Structural basis for the recognition of regulatory subunits by the catalytic subunit of protein phosphatase 1. *EMBO J.* **16**, 1876-1887.

Feng, Z. H., Wilson, S. E., Peng, Z. Y., Schlender, K. K., Reimann, E. M. and Trumbly, R. J. (1991). The yeast *GLC7* gene required for glycogen accumulation encodes a type 1 protein phosphatase. *J. Biol. Chem.* **266**, 23796-23801.

Francisco, L., Wang, W. F. and Chan, C. S. M. (1994). Type 1 protein phosphatase acts in opposition to Ipl1 protein kinase in regulating yeast chromosome segregation. *Mol. Cell. Biol.* **14**, 4731-4740.

François, J. M., Thompson-Jaeger, S., Skroch, J., Zellenka, U., Spevak, W. and Tatchell, K. (1992). *GAC1* may encode a regulatory subunit for protein phosphatase type 1 in *Saccharomyces cerevisiae*. *EMBO J.* **11**, 87-96.

Frederick, D. L. and Tatchell, K. (1996). The *REG2* gene of *Saccharomyces cerevisiae* encodes a type 1 protein phosphatase-binding protein that functions with Reg1p and the Snf1 protein kinase to regulate growth. *Mol. Cell. Biol.* **16**, 2922-2931.

Gietz, R. D. and Sugino, A. (1988). New yeast-*Escherichia coli* shuttle vectors constructed with *in vitro* mutagenised yeast genes lacking six-base pair restriction sites. *Gene* **74**, 527-534.

Gietz, R. D., St Jean, A., Woods, R. A. and Schiestl, R. H. (1992). Improved method for high efficiency transformation of intact yeast cells. *Nucleic Acids Res.* **20**, 1425.

Hake, S. B., Masternak, K., Kammerbauer, C., Janzen, C., Reith, W. and Steimle, V. (2000). CIITA leucine-rich repeats control nuclear localization, In vivo recruitment to the major histocompatibility complex (MHC) class II enhanceosome, and MHC class II gene transactivation. *Mol. Cell. Biol.* **20**, 7716-7725.

Hisamoto, N., Frederick, D. L., Sugimoto, K., Tatchell, K. and Matsumoto,

K. (1995). The *EGP1* gene may be a positive regulator of protein phosphatase type 1 in the growth control of *Saccharomyces cerevisiae*. *Mol. Cell. Biol.* **15**, 3767-3776.

Hong, G., Trumbly, R. J., Reimann, E. M. and Schlender, K. K. (2000). Sds22p is a subunit of a stable isolatable form of protein phosphatase 1 (Glc7p) from *Saccharomyces cerevisiae*. *Arch. Biochem. Biophys.* **376**, 288-298.

Hsu, J.-Y., Sun, Z.-W., Li, X., Reuben, M., Tatchell, K., Bishop, D. K., Grushcow, J. M., Brame, C. J., Caldwell, J. A., Hunt, D. F. et al. (2000). Mitotic phosphorylation of histone H3 is governed by Ipl1/aurora kinase and Glc7/PP1 phosphatase in budding yeast and nematodes. *Cell* **102**, 279-291.

Hubbard, M. J. and Cohen, P. (1989). The glycogen-binding subunit of protein phosphatase1_G from rabbit skeletal muscle. Further characterisation of its structure and glycogen-binding properties. *Eur. J. Biochem.* **180**, 457-465.

Hubbard, M. J. and Cohen, P. (1993). On target with a new mechanism for the regulation of protein phosphorylation. *Trends Biochem. Sci*. **18**, 172-177.

Jiang, H., Tatchell, K., Liu, S. and Michels, C. A. (2000). Protein phosphatase type 1 regulatory subunits Reg1p and Reg2p act as signal transducers in the glucose-induced inactivation of maltose permease in *Saccharomyces cerevisiae*. *Mol. Gen. Genet.* **263**, 411-422.

Kaiser, C., Michaelis, S. and Mitchell, A. (1994). Methods in Yeast Genetics. A Cold Spring Harbour Laboratory Course Manual. New York: Cold Spring Harbor Laboratory Press.

Kalderon, D., Roberts, B. L., Richardson, W. D. and Smith, A. E. (1984). A short amino acid sequence able to specify nuclear location. *Cell* **39**, 499-509.

Kobe, B. and Deisenhofer, J. (1994). The leucine-rich repeat: a versatile binding motif. *Trends Biochem. Sci.* **19**, 415-421.

Kreivi, J. P., Trinkle-Mulcahy, L., Lyon, C. E., Morrice, N. A., Cohen, P. and Lamond, A. I. (1997). Purification and characterisation of p99, a nuclear modulator of protein phosphatase 1 activity. *FEBS Lett.* **420**, 57-62.

Lau, D., Kunzler, M., Braunwarth, A., Hellmuth, K., Podtelejnikov, A., Mann, M. and Hurt, E. (2000). Purification of protein A-tagged yeast ran reveals association with a novel karyopherin beta family member, Pdr6p. *J. Biol. Chem.* **275**, 467-471.

MacKelvie, S. H., Andrews, P. D. and Stark, M. J. R. (1995). The *Saccharomyces cerevisiae* gene *SDS22* encodes a potential regulator of the mitotic function of yeast type 1 protein phosphatase. *Mol. Cell. Biol.* **15**, 3777-3785.

Michaelis, C., Ciosk, R. and Nasmyth, K. (1997). Cohesins: chromosomal proteins that prevent premature separation of sister chromatids. *Cell* **91**, 35-45.

Morrice, N. A. and Powis, S. J. (1998). A role for the thiol-dependent reductase ERp57 in the assembly of MHC class I molecules. *Curr. Biol.* **8**, 713-716.

Ohkura, H. and Yanagida, M. (1991). *S. pombe* gene *sds22*$^+$ essential for a midmitotic transition encodes a leucine-rich repeat protein that positively modulates protein phosphatase 1. *Cell* **64**, 149-157.

Peters, C., Andrews, P. D., Stark, M. J., Cesaro-Tadic, S., Glatz, A., Podtelejnikov, A., Mann, M. and Mayer, A. (1999). Control of the terminal step of intracellular membrane fusion by protein phosphatase 1. *Science* **285**, 1084-1087.

Rayner, J. C. and Munro, S. (1998). Identification of the MNN2 and MNN5 mannosyltransferases required for forming and extending the mannose branches of the outer chain mannans of *Saccharomyces cerevisiae*. *J. Biol. Chem.* **273**, 26836-26843.

Renouf, S., Beullens, M., Wera, S., Van Eynde, A., Sikela, J., Stalmans, W. and Bollen, M. (1995). Molecular cloning of a human polypeptide related to yeast Sds22, a regulator of protein phosphatase 1. *FEBS Lett.* **375**, 75-78.

Robbins, J., Dilworth, S. M., Laskey, R. A. and Dingwall, C. (1991). Two interdependent basic domains in nucleoplasmin nuclear targeting sequence: identification of a class of bipartite nuclear targeting sequence. *Cell* **64**, 615-623.

Sambrook, J., Fritsch, E. F. and Maniatis, T. (1989). Molecular Cloning. A Laboratory Manual. New York: Cold Spring Harbor Laboratory Press.

Sassoon, I., Severin, F. F., Andrews, P. D., Taba, M. R., Kaplan, K. B., Ashford, A. J., Stark, M. J., Sorger, P. K. and Hyman, A. A. (1999). Regulation of *Saccharomyces cerevisiae* kinetochores by the type 1 phosphatase Glc7p. *Genes Dev.* **13**, 545-555.

Siegel, L. M. and Monty, K. J. (1966). Determination of molecular weights and frictional ratios of proteins in impure systems by use of gel filtration and density gradient centrifugation. Application to crude preparations of sulfite and hydroxylamine reductases. *Biochim. Biophys. Acta* **112**, 346-362.

Sikorski, R. S. and Boeke, J. D. (1991). *In vitro* mutagenesis and plasmid shuffling. From cloned gene to mutant yeast. *Methods Enzymol.* **194**, 302-318.

Sikorski, R. S. and Hieter, P. (1989). A system of shuttle vectors and yeast host strains designed for efficient manipulation of DNA in *Saccharomyces cerevisiae*. *Genetics* **122**, 19-27.

Sillekens, P. T., Beijer, R. P., Habets, W. J. and van Verooij, W. J. (1989). Molecular cloning of the cDNA for the human U2 snRNA-specific A' protein. *Nucleic Acids Res.* **17**, 1893-1906.

Spencer, F., Gerring, S. L., Connelly, C. and Hieter, P. (1990). Mitotic chromosome transmission fidelity mutants in *Saccharomyces cerevisiae*. *Genetics* **124**, 237-249.

Stark, M. J. R. (1996). Yeast protein serine/threonine phosphatases: multiple roles and diverse regulation. *Yeast* **12**, 1647-1675.

Stark, M. J. R. (1998). Studying essential genes: generating and using promoter fusions and conditional alleles. In *Yeast Gene Analysis* (Vol. 26) (ed. A. J. P. Brown and M. F. Tuite), pp. 83-99. London: Academic Press.

Stirling, D. A., Welch, K. A. and Stark, M. J. R. (1994). Interaction with calmodulin is required for the function of Spc110p, an essential component of the yeast spindle pole body. *EMBO J.* **13**, 4329-4342.

Stone, E. M., Yamano, H., Kinoshita, N. and Yanagida, M. (1993). Mitotic regulation of protein phosphatases by the fission yeast sds22 protein. *Curr. Biol.* **3**, 13-26.

Stuart, J. S., Frederick, D. L., Varner, C. M. and Tatchell, K. (1994). The mutant type 1 protein phosphatase encoded by *glc7-1* from *Saccharomyces cerevisiae* fails to interact productively with the *GAC1*- encoded regulatory subunit. *Mol. Cell. Biol.* **14**, 896-905.

Tu, J. and Carlson, M. (1994). The GLC7 type 1 protein phosphatase is required for glucose repression in *Saccharomyces cerevisiae*. *Mol. Cell. Biol.* **14**, 6789-6796.

Tu, J. and Carlson, M. (1995). REG1 binds to protein phosphatase type 1 and regulates glucose repression in *Saccharomyces cerevisiae*. *EMBO J.* **14**, 5939-5946.

Tu, J., Song, W. and Carlson, M. (1996). Protein phosphatase type 1 interacts with proteins required for meiosis and other cellular processes in *Saccharomyces cerevisiae*. *Mol. Cell. Biol.* **16**, 4199-4206.

Uetz, P., Giot, L., Cagney, G., Mansfield, T. A., Judson, R. S., Knight, J. R., Lockshon, D., Narayan, V., Srinivasan, M., Pochart, P. et al. (2000). A comprehensive analysis of protein-protein interactions in *Saccharomyces cerevisiae*. *Nature* **403**, 623-627.

Van Eynde, A., Wera, S., Beullens, M., Torrekens, S., Van Leuven, F., Stalmans, W. and Bollen, M. (1995). Molecular cloning of NIPP-1, a nuclear inhibitor of protein phosphatase 1, reveals homology with polypeptides involved in RNA processing. *J. Biol. Chem.* **270**, 28068-28074.

Waddle, J. A., Karpova, T. S., Waterston, R. H. and Cooper, J. A. (1996). Movement of cortical actin patches in yeast. *J. Cell Biol.* **132**, 861-870.

Wu, X. and Tatchell, K. (2001). Mutations in yeast protein phosphatase type 1 that affect targeting subunit binding. *Biochemistry* **40**, 7410-7420.

Yoon, H. J. and Carbon, J. (1999). Participation of Bir1p, a member of the inhibitor of apoptosis family, in yeast chromosome segregation events. *Proc. Natl. Acad. Sci. USA* **96**, 13208-13213.

Zhao, S. and Lee, E. Y. (1997). A protein phosphatase 1-binding motif identified by the panning of a random peptide display library. *J. Biol. Chem.* **272**, 28368-28372.